ACS APPLIED MATERIALS & INTERFACES

Research Article

www.acsami.org

Panchromatic Donor–Acceptor–Donor Conjugated Oligomers for Dye-Sensitized Solar Cell Applications

Romain Stalder,[†] Dongping Xie,[†] Ashraful Islam,[§] Liyuan Han,[§] John R. Reynolds,*[,†,‡] and Kirk S. Schanze*[,†]

[†]Department of Chemistry, Center for Macromolecular Science and Engineering, University of Florida, Gainesville, Florida 32611, United States

[§]Photovoltaic Materials Unit, National Institute for Materials Science, Sengen 1-2-1, Tsukuba, Ibaraki 305-0047, Japan

[‡]School of Chemistry and Biochemistry, School of Materials Science and Engineering, Center for Organic Photonics and Electronics, Georgia Institute of Technology, Atlanta, Georgia 30332, United States

Supporting Information

ABSTRACT: We report on a sexithienyl and two donor–acceptor–donor oligothiophenes, employing benzothiadiazole and isoindigo as electron-acceptors, each functionalized with a phosphonic acid group for anchoring onto TiO_2 substrates as light-harvesting molecules for dye sensitized solar cells (DSSCs). These dyes absorb light to wavelengths as long as 700 nm, as their optical HOMO/LUMO energy gaps are reduced from 2.40 to 1.77 eV with increasing acceptor strength. The oligomers were adsorbed onto mesoporous TiO_2 films on fluorine doped tin oxide (FTO)/glass substrates and incorporated into DSSCs, which show AM1.5 power conversion efficiencies (PCEs) ranging between 2.6% and 6.4%. This work demonstrates that the donor–acceptor–donor (D-A-D) molecular structures coupled to phosphonic acid anchoring groups, which have not been used in DSSCs, can lead to high PCEs.

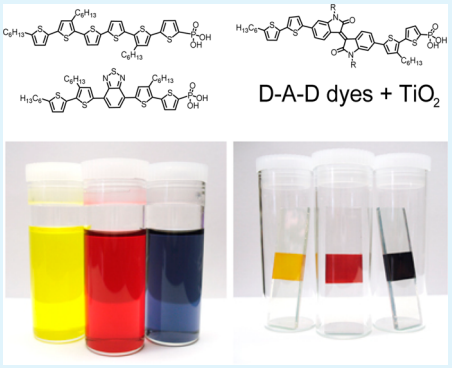

KEYWORDS: *isoindigo, benzothiadiazole, phosphonate anchoring group, dye sensitized solar solar cell, donor-acceptor chromophore, conjugated oligomer*

INTRODUCTION

Dye-sensitized solar cells (DSSC) are one of the most important emerging photovoltaic technologies. Since the first report of the DSSC by Grätzel and co-workers in 1991,[1] the technology has seen increasing research interest directed to the understanding of fundamental problems and to the exploration of opportunities for commercialization.[2] Compared to traditional solid-state solar cells, the advantages of the DSSC format include the use of relatively inexpensive materials, the possibility that mechanically flexible modules can be deployed on a large scale for low overall cost, and as the dyes employed can have controllable light absorption properties, the cells can be made in a variety of aesthetically pleasing colors and levels of transmissivity.[3] Considerable success has been achieved with DSSCs that rely upon metal complexes as the visible light absorbing sensitizers. Ruthenium-based polypyridyl sensitizers have led the field early on, with power conversion efficiencies (PCEs) now up to 11.5%,[4,5] while Zn-centered porphyrins recently achieved even higher PCE of 12.3%.[6,7] Phthalocyanines are another class of popular dyes that have been extensively studied for DSSCs, reaching PCEs close to 6.0%.[8]

Metal-free organic molecular dyes as alternative sensitizers have also attracted research attention due to a number of potential advantages ranging from the control of structure organic compounds bring, to the access to inexpensive and environmentally benign resources, high light absorptivity, and facile synthesis. To date, hundreds of organic dyes have been evaluated as sensitizers and the highest efficiency cells have achieved comparable PCEs (> 10%) as those with metal-based dyes.[9,10] Recently, perovskite based cells have pushed these PCE values to over 15%.[11−13] Generally, the design of the organic dyes utilizes a donor–π-bridge–acceptor (D-π-A) type of structure, which is believed to facilitate intramolecular charge transfer (ICT) from donor, to acceptor, to the TiO_2 interface via the π-conjugated linker. In a majority of these D-π-A structures, the donor unit is a derivative of the triarylamine moiety, such as triphenylamine (TPA), while the acceptor unit is the commonly used cyanoacrylic acid group, which also serves as an anchoring group.[10]

In comparison, symmetrically structured sensitizers based on donor–acceptor-donor (D-A-D) configurations have received far less attention, presumably because the symmetry of the π-electron distribution is expected to disrupt the vectorial spatial/energetic orientation between the dye and the TiO_2 interface and conduction band—potentially hampering charge transfer. In contrast, symmetrical D-A-D type conjugated oligomers have

Received: March 13, 2014
Accepted: April 21, 2014
Published: May 7, 2014

   dx.doi.org/10.1021/am501515s | ACS Appl. Mater. Interfaces 2014, 6, 8715−8722

Scheme 1. Structure of the Three Dyes Used in This Study, T6-A, T4BTD-A, and T4iI-A, along with Synthesis of the Isoindigo-Based Dye T4iI-A

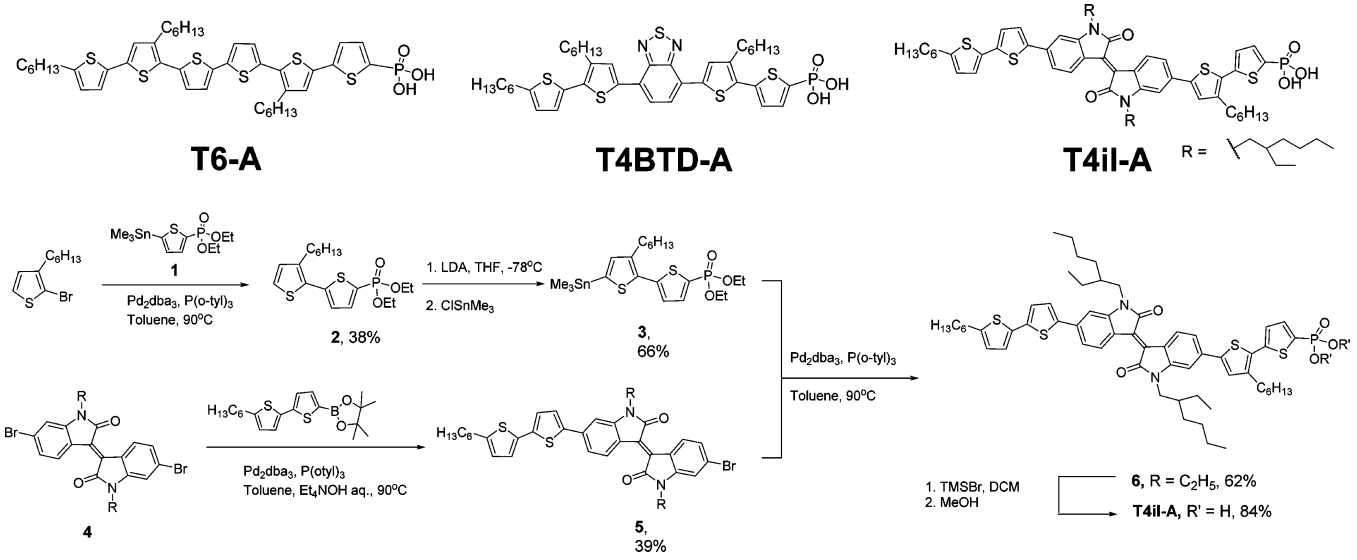

been widely studied for solid-state organic photovoltaic and organic field effect transistor applications.[14,15] Towards this objective, we have reported on a series of D-A-D conjugated molecules with tailored absorption profiles and controlled energies of the frontier molecular orbitals (FMO) by systematically varying the electron-donating and electron-withdrawing strength of the D and A units, respectively.[16]

Herein, we demonstrate the use of visible light absorbing π-conjugated oligomers which feature a D-A-D type electronic structure, combined with phosphonic acid anchoring groups, for n-type DSSC sensitization. Importantly, our molecular design diverges from the commonly employed D-π-A structure since we are not using strongly electron-withdrawing groups such as cyanoacrylic acid at the binding end of the molecule. Although the carboxylic acid functionality is most commonly employed as anchoring group in DSSCs, the use of phosphonic acid has also been studied as an alternative, first reported for efficient DSSCs by Péchy and coworkers for a Ru-based system,[17] followed by several other examples of metal-based molecules[18−27] and D-π-A molecules.[28−30] Compared to carboxylic acids, phosphonic acids have been reported to enhance the strength and chemical stability of dye adsorption onto TiO_2 surfaces.[31−33] Specifically, we have designed and synthesized three thiophene-based discrete-length oligomers unsymmetrically functionalized with one phosphonic acid group. The conjugated systems were varied from an all-thiophene seximer (T6-A) to D-A-D structures incorporating benzothiadiazole (BTD) and 6,6′-isoindigo (iI)[34] as electron-deficient (acceptor) cores flanked with two bithiophene (donor) units (T4BTD-A and T4iI-A, respectively). Mirroring their absorption profiles, incident photon-to-current conversion efficiency (IPCE) results indicate the dyes sensitize TiO_2 to wavelengths in the order T6-A > T4BTD-A > T4iI-A, with the BTD derivative showing the highest plateau in efficiency near 80% and exhibiting a promising AM 1.5 DSSC performance exceeding 6% PCE.

EXPERIMENTAL SECTION

Oligomer Synthesis and Characterization. The synthesis and characterization of T6-A and T4BTD-A is reported elsewhere.[35] Complete details concerning the synthesis and spectroscopic characterization of T4iI-A are provided in the Supporting Information.

Cell Fabrication and Characterization. A double-layer TiO_2 photoelectrode (thickness 15 μm; area 0.25 cm^2) was used as a working electrode. A 10 μm main transparent layer with titania particles (~20 nm) and a 5 μm scattering layer with titania particles (~400 nm) were screen-printed on fluorine-doped tin oxide (FTO) conducting glass substrate.[36] The thickness of the films was measured with a Surfcom 1400A surface profiler (Tokyo Seimitsu Co. Ltd.). The films were further treated with 0.1 M HCl aqueous solutions before examination.[37] Solutions (3×10^{-4} M) of T6-A or T4iI-A in dichlorobenzene and T4BTD-A in acetonitrile/*tert*-butyl alcohol (1/1, v/v) were used to coat the TiO_2 film with the dyes. Deoxycholic acid (20 mM) was added to the dye solution as a co-adsorbent to prevent aggregation of the dye molecules. The electrodes were immersed in the dye solutions and then kept at 25°C for 24 h to adsorb the dye onto the TiO_2 surface. Photovoltaic measurements were performed in a two-electrode sandwich-type sealed-cell configuration. The dye-coated TiO_2 film was used as the working electrode, and platinum-coated conducting glass was used as the counter-electrode. The two electrodes were separated by a Surlyn spacer (50 μm thick) and sealed up by heating the polymer frame. The DSSC performances of all three dyes were tested using the following electrolyte composition (electrolyte 1): 0.6 M dimethylpropylimidazolium iodide (DMPII), 0.05 M I_2, 0.1 M LiI, and 0.5 M *tert*-butylpyridine (TBP) in acetonitrile. In the case of T4iI-A, two other electrolyte compositions were tested, as follows: 0.6 M dimethylpropylimidazolium iodide (DMPII), 0.05 M I_2, and 0.1 M LiI in acetonitrile (electrolyte 2) and 0.6 M dimethylpropylimidazolium iodide (DMPII), 0.05 M I_2, and 0.5 M LiI in acetonitrile (electrolyte 3). The current−voltage characteristics were measured under standard AM 1.5 sunlight (100 mW cm^{-2}, WXS-155S-10: Wacom Denso Co. Japan). Incident photon-to-current conversion efficiency spectra were measured with monochromatic incident light of 1×10^{16} photons cm^{-2} under 100 mW cm^{-2} in director current mode (CEP-2000BX, Bunko-Keiki).

RESULTS AND DISCUSSION

Monofunctional Oligothiophene Synthesis. Scheme 1 shows the structures of the three asymmetric phosphonic acid functionalized dyes employed. We recently reported the synthesis of T6-A and T4BTD-A,[35] and that of T4iI-A follows a similar synthetic strategy as described in Scheme 1. First, a thiophene ring was phosphonated at the 2-position and subsequently stannylated at the 5-position, leading to

compound **1** as previously reported.[35] This was reacted with 2-bromo-3-hexylthiophene under Stille coupling conditions in toluene to afford the phosphonated bithiophene **2** in moderate yield. The catalytic system used throughout the synthesis was based on Pd(0) in the form of tris(dibenzylideneacetone) dipalladium, to which was added tri(*o*-tolyl)phosphine as ligand. Deprotonation of the alkylthiophene ring of **2** at the 5-position using LDA at low temperature followed by quenching of the anion with trimethyltin chloride yielded the stannylated product **3**. Prior to conjugation extension, the isoindigo unit **4** was *N*-alkylated with 2-ethylhexyl side chains for solubility purposes.

The core of the aromatic system of T4iI-A was then extended asymmetrically by reacting the 6,6′-dibromoisoindigo derivative **4** with one equivalent of 2-(5′-hexyl-[2,2′-bithiophen]-5-yl)-4,4,5,5-tetramethyl-1,3,2-dioxaborolane under Suzuki coupling conditions. The catalytic system was the same as for the Stille couplings with the addition of a 1 M tetraethylammonium hydroxide aqueous solution as a base. Upon completion of the reaction, the remaining starting material and the di-coupled by-product were separated from the mono-coupled product by column chromatography, affording unsymmetrical compound **5** in 38% yield. The remaining haloaryl position on **5** was then reacted with stannylated bithiophene **3** under the same Stille coupling conditions, leading to the isoindigo-based D-A-D oligothiophene **6** functionalized with a diethyl phosphonate group. In a final step, the latter group was converted to its phosphonic acid in the presence of bromotrimethylsilane followed by quenching with methanol. With the T4iI-A phosphonic acid on hand, its optical and electrochemical properties were measured and compared to that of the T6-A and T4BTD-A oligothiophenes.

Optical and Electrochemical Properties. The absorption spectra of the three dyes were recorded in chloroform solution, as displayed in Figure 1 and summarized in Table 1. The molar absorptivities (ε) of the dyes were measured between 20 000 and 50 000 M^{-1} cm^{-1} at their respective peak wavelength absorption maxima (see Supporting Information Figure S1). The absorption profile of T6-A is a single band centered at 426 nm, with a low-energy onset at 515 nm, which corresponds to a HOMO-LUMO optical energy gap of 2.40 eV. The D-A-D oligothiophenes both display a two-band absorption profile, peaking at 360 and 504 nm for T4BTD-A and at 360 and 580 nm for T4iI-A. This is consistent with the effect of donor−acceptor interaction on the π-electron system,[38] with the prominence of the intramolecular charge transfer band at higher wavelengths. For T4BTD-A, the intensity of the absorption gap between the two absorption maxima decreases to 30% of the low-energy band maximum, which is more pronounced than for T4iI-A, for which the absorption gap intensity decreases to 52% of the low-energy absorption maximum. As the transmission window for both compounds is near 400 nm and the high energy peak is in the UV, the colors expressed by these two D-A-D compounds is dominated by the absorption due to the charge transfer transitions. The spectra span the visible spectrum, from yellow (T6-A) to red (T4BTD-A) to blue (T4iI-A) with absorption onsets of 515, 608, and 702 nm, respectively, corresponding to HOMO-LUMO optical energy gaps reducing from 2.40 to 1.77 eV.

Each dye was adsorbed onto a titania nanoparticle film by dipping the latter into a DMF solution of the compound for 3 h and washing the sensitized films with DMF and ethanol. A photo of each film is shown in Figure 1b, and their absorbance

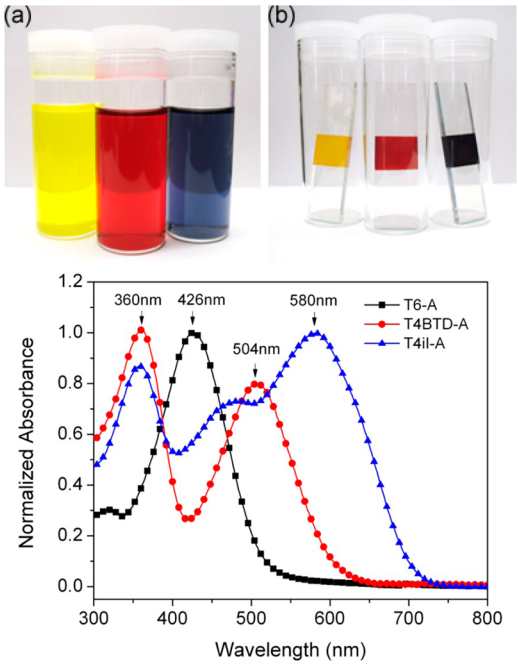

Figure 1. Normalized absorption spectra of T6-A, T4BTD-A, and T4iI-A in $CHCl_3$ solution, and picture of T6-A, T4BTD-A, and T4iI-A in DMF solution (a, left to right) and adsorbed onto TiO_2 (b, left to right).

spectra are displayed in the Supporting Information. The spectral results demonstrate the panchromatic absorption achieved in both solution and adsorbed films—promising for their use as dyes for DSSCs.

The photoluminescence maxima of T6-A and T4BTD-A, which we previously reported for dilute chloroform solutions,[35] are red-shifted from 565 nm for the former to 676 nm for the latter, with fluorescence quantum efficiencies of 49% and 71%, respectively. Their fluorescence lifetimes were measured at 0.85 ns for T6-A and 5.5 ns for T4BTD-A. Sensitizers with longer fluorescence lifetimes are particularly attractive as this increases the probability for charge separation of the photogenerated exciton, therefore favoring electron injection into the conduction band of the TiO_2 film. In contrast, the fluorescence intensity of the isoindigo-based molecule T4iI-A was very low regardless of the excitation wavelength, with a quantum efficiency lower than 0.1% and a singlet lifetime <100 ps. This photophysical trait is consistent amongst all iI-based conjugated materials, and unfortunately has yet to be fully understood.[39]

In order to evaluate the energy of the HOMO and LUMO levels of each dye, their electrochemistry was studied in solution, all potentials being referenced against Fc/Fc^+. The CVs and DPVs for each molecule dissolved at 1 mM in a DCM electrolyte containing 0.1 M $TBAPF_6$ were recorded, as reported previously for T6-A and T4BTD-A,[35] and displayed in Figure 2a for T4iI-A. Table 1 provides a listing of the onset potentials and corresponding HOMO and LUMO energies. The CV of the isoindigo derivative shows two quasi-reversible reduction processes, centered at half-wave potentials between −1.26 V and −1.68 V, while two overlapping oxidation waves could be distinguished at 0.55 and 0.66 V. From the onsets of oxidation and reduction, measured at 0.45 V and −1.15 V, respectively, we calculated the HOMO and LUMO levels of T4iI-A to be at −5.55 eV and −3.95 eV versus vacuum. This

dx.doi.org/10.1021/am501515s | ACS Appl. Mater. Interfaces 2014, 6, 8715−8722

Table 1. Optical and Electrochemical Properties of the Dyes in Solution

dye	λ_{max} (nm)	ΔE^{opt} (eV)	ε (M^{-1} cm^{-1})	E_{ons}^{ox} (V)[b]	E_{ons}^{red} (V)[b]	E_{HOMO} (eV)	E_{LUMO} (eV)
T6-A[a]	426	2.40	48 700	0.20		5.30	2.90
T4BTD-A[a]	504	2.04	21 000	0.40	−1.55	5.50	3.55
T4iI-A	580	1.77	37 500	0.45	−1.15	5.55	3.95

[a]Results from ref 35. [b]Calibrated against the Fc/Fc^+ redox standard, set at −5.1 eV vs. vacuum.[40−42]

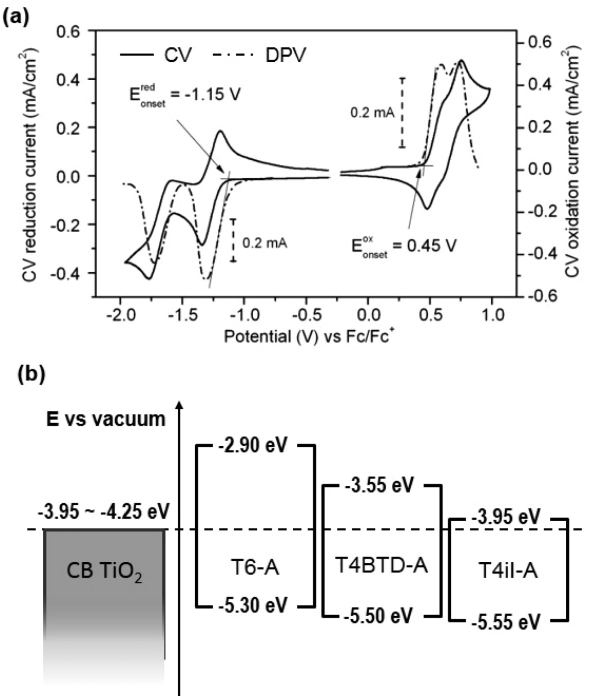

Figure 2. (a) Cyclic and differential pulse voltammograms of a T4iI-A solution in 0.1M $TBAPF_6/CH_2Cl_2$, recorded at 50 mV/s. (b) Energy levels diagram depicting the position of the HOMO and LUMO levels of T6-A, T4BTD-A, and T4iI-A with respect to the conduction band of TiO_2.

was done by setting the Fc/Fc^+ redox standard at −5.1 eV versus vacuum, since Fc/Fc^+ is +0.4 V vs. SCE,[40] and the energy of SCE is −4.7 eV vs vacuum.[41,42] By analogy, the HOMO and LUMO energies of T4BTD-A were measured from DPV to be at −5.50 eVand −3.55 eV, respectively. The HOMO energy of T6-A was accessible by DPV, and measured at −5.30 eV, but the LUMO had to be calculated using the value of the optical HOMO-LUMO gap. These results confirm that as electron-deficient units are used in the D-A-D structure, the energy gaps are reduced for T4BTD-A and T4iI-A as a result of deeper LUMO energy levels (higher electron affinities). The stronger electron-accepting character of isoindigo decreases the LUMO to −3.95 eV, more than 1.0 eV deeper than for the sexithiophene dye and 0.4 eV deeper than for the BTD-based dye.

Figure 2b shows a comparison of these energy levels with that of the TiO_2 conduction band (E_{CB}). The values for TiO_2 are approximate since the chemical environment—such as pH or bound species—at the TiO_2 surface can affect the E_{CB} by several hundreds of meV.[2,43] For instance, it is reported that the TiO_2 rutile E_{CB} can range from −0.05 V at pH 2 to −0.6 V at pH 6 vs NHE, and that the anatase E_{CB} at pH 2 is found at −0.28 V vs NHE.[44] This corresponds to an E_{CB} range of −4.4 eV to −3.85 eV, since NHE is at −4.45 eV,[41] although the commonly accepted values in the DSSC literature for TiO_2 E_{CB} are found between −0.2 and −0.5 V vs NHE, that is, between −4.25 and −3.95 eV.[10,45,46] Furthermore, adsorbed phosphonic acid functionalized dyes or additives have been reported to influence the DSSC photovoltaic parameters as a result of shifting the E_{CB} of TiO_2 depending on the molecule's dipole moment.[47,48] Nevertheless, the energy diagram in Figure 2b clearly depicts that as the energy gap of the dyes is decreased, the LUMO energy approaches that of the conduction band of TiO_2. In particular, the LUMO energy of the T4iI-A dye at −3.95 eV could be close to the E_{CB} of TiO_2 depending on the latter's accepted value, which may limit the efficiency of the electron injection into the TiO_2 film.

Dye-Sensitized Solar Cells. Each DSSC was constructed by soaking a screen-printed TiO_2 nanoparticle film (0.25 cm^2 onto FTO/glass substrate) into a dye solution containing deoxycholic acid as additive to prevent aggregation of the adsorbed dye. The photoelectrode was then sealed against a Pt-coated glass counter electrode separated with an electrolyte-soaked membrane. The photovoltaic performance was then measured under standard AM 1.5 sunlight (100 mW cm^{-2}). Full details of the solar cell fabrication can be found in the

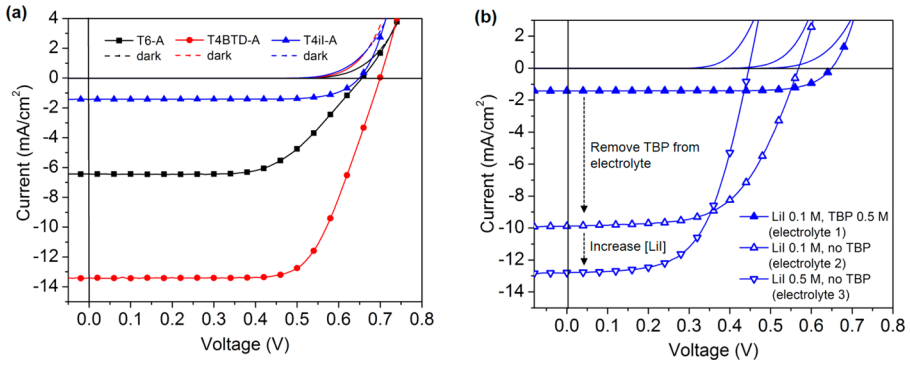

Figure 3. (a) *I*−*V* curves of the DSSCs using T6-A, T4BTD-A, and T4iI-A dyes in electrolyte 1 under AM1.5 illumination (100 mW cm^{-2}), and (b) evolution of the *I*−*V* curves of the T4iI-A cells using electrolytes 1, 2, and 3.

Table 2. PV Parameters of the DSSCs Based on T6-A, T4BTD-A, and T4iI-A[a]

dye	electrolyte	composition	J_{sc} (mA/cm^2)	V_{oc} (V)	FF (%)	PCE (%)
T6-A	1	LiI 0.1 M, TBP 0.5 M	6.43	0.66	61	2.56
T4BTD-A	1	LiI 0.1 M, TBP 0.5 M	13.4	0.70	68	6.40
T4iI-A	1	LiI 0.1 M, TBP 0.5 M	1.42	0.64	76	0.69
T4iI-A	2	LiI 0.1 M, no TBP	9.89	0.57	59	3.30
T4iI-A	3	LiI 0.5 M, no TBP	12.8	0.45	59	3.39

[a]All cells measured with 0.05 M I_2 in the electrolyte, under AM1.5 illumination (100 mW cm^{-2}).

Experimental section. Figure 3a shows the current−voltage (I−V) characteristics of each cell recorded under identical conditions using electrolyte 1.

As summarized in Table 2, a moderate short-circuit current (J_{sc}) of 6.43 mA/cm^2 was recorded for the T6-A-based cell, while that of the T4BTD-A was the highest at 13.4 mA/cm^2. For the cell based on T4iI-A a low J_{sc} of 1.42 mA/cm^2 was recorded. The open-circuit voltage (V_{oc}) of the T4iI-A cell is the lowest, at 0.64 V, while that of the T6-A cell at 0.66 V approaches that of the T4BTD-A cell, which is the highest at 0.70 V. With high fill factors (FF) between 61% and 76%, this results in a moderate power conversion efficiency (PCE) of 2.56% for the T6-A cell, and a low PCE of 0.69% for the T4iI-A cell, while the T4BTD-A cell achieved a high PCE of 6.40%.

To further investigate the low performance of T4iI-A, DSSC cells with varied electrolyte composition were also fabricated. In electrolyte 1 the LiI concentration was 0.1 M with the presence of 0.5 M TBP. In electrolyte 2, the concentration of LiI was kept at 0.1 M, but TBP was not added to the electrolyte. In electrolyte 3, the concentration of LiI was increased from 0.1 to 0.5 M, still without the presence of TBP, as shown in Table 2. The I−V characteristics of the three T4iI-A cells are also displayed in Table 2 and in Figure 3b.

When TBP was removed from the electrolyte composition (electrolyte 2), the J_{sc} dramatically increased to 9.89 mA/cm^2, at the expense of the V_{oc}, which decreased to 0.57 V. The FF also decreased to 59 %, but the overall increase in current resulted in a five-fold increase in PCE to 3.30 %. When the LiI concentration was increased from 0.1 to 0.5 M (electrolyte 3), the J_{sc} increased to 12.8 mA/cm^2, which is comparable to that of T4BTD-A, but the V_{oc} decreased further to 0.45 V. With identical FF for both concentrations, this only improved the PCE of the T4iI-A cell to 3.39 %.

The difference in PCE between the three dyes is reflected in the IPCE spectra displayed in Figure 4, which shows the photocurrent action spectra for the T6-A and T4BTD-A cells as well as the best cell for T4iI-A. The IPCE of the T6-A and T4BTD-A cells peak at 73% and 81% respectively. Consistent with the broader absorption of D-A-D oligothiophenes, more extended current generation up to 680 nm is observed for T4BTD-A cells compared to the T6-A cells for which the IPCE drops at 550 nm. Likewise, the IPCE of the broadest absorbing cell based on T4iI-A records current generation up to 750 nm, but the intensity is lower than that of the other two dyes, as the current is confined below 55% for the best T4iI-A cell. The evolution of the IPCE for T4iI-A-based cells depending on the electrolyte composition can be found in the Supporting Information.

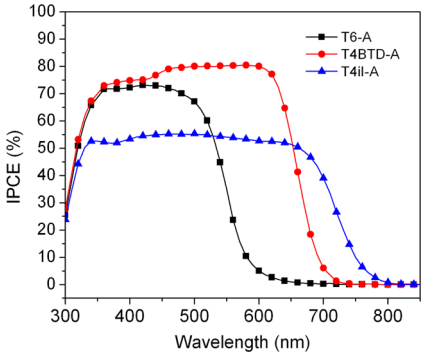

Figure 4. Incident photon-to-current conversion efficiency (IPCE) of the DSSCs based on T6-A and T4BTD-A in electrolyte 1 and T4iI-A in electrolyte 3.

DISCUSSION

Performance of Isoindigo Dye. In this study, we measured the DSSC performance of the isoindigo-based dye T4iI-A under the same conditions (electrolyte 1) as for T6-A and T4BTD-A, and found a limited PCE of 0.69 %. This is a result of a low J_{sc} of 1.42 mA/cm^2, which is unfortunate given the extended absorption of the dye towards the NIR. In comparison, T4BTD-A showed a high J_{sc} of 13.4 mA/cm^2 under otherwise identical D-A-D dye design and experimental conditions. This low current is likely due to an inefficient electron transfer from T4iI-A to TiO_2, and suggests that changing the acceptor from BTD to iI in the D-A-D structure brings the LUMO of the dye too close to the CB of TiO_2, when electrolyte 1 is used.

The additive TBP, which was added in electrolyte 1 but not in electrolytes 2 and 3, is reported to increase the lifetime of injected electrons in TiO_2 and to raise the conduction band of TiO_2 (and thus increase the V_{oc}).[49] Consequently, it is now widely used in the field to increase DSSCs efficiencies.[2] For T4iI-A, we observed a decrease in V_{oc} from 0.64 to 0.57 V when TBP was *removed* from the electrolyte, suggesting that the CB of TiO_2 is lower in electrolyte 2, which is consistent with the reported effect of the additive. As shown in Table 2, removing the additive had a more striking effect on the J_{sc}, which was increased by seven-fold to 9.89 mA/cm^2, resulting in a PCE of 3.30 %. If one considers that the LUMO level of T4iI-A is 0 to 0.3 eV higher than the conduction band of TiO_2 (depending on the accepted value for TiO_2 E_{CB}, see Figure 2b), then it is not surprising that lowering the conduction band of TiO_2 as a result of removing TBP from the electrolyte would result in more efficient electron injection and thus dramatically higher J_{sc}. A similar effect of TBP on J_{sc} has been observed for DSSCs where the dye had a low-lying LUMO.[50−52] In electrolyte 3, the concentration of LiI was increased from 0.1 to 0.5 M. As the concentration of LiI is increased, it is likely that more cations reach and adsorb onto (or intercalate into) the surface of TiO_2,[53,54] which then shifts the potential of the conduction band positively (lowers the conduction band with respect to vacuum). This is consistent with the further decrease in the V_{oc} from 0.57 V at 0.1 M LiI (electrolyte 2) to 0.45 V at 0.5 M LiI

(electrolyte 3). The same trend was described in a recent study with the dye N719, where the [LiI]/[I_2] ratio was increased from 2:1 to 10:1 at various [I_2] including 0.05 M, which corresponds to our experimental conditions.[55] The J_{sc} further increased to 12.8 mA/cm^2, which is consistent with an even more efficient electron injection into the TiO_2 film. Overall, this suggests that the T4iI-A LUMO energy is at the threshold of the required energetic offset (~0.2 eV)[2] with respect to the E_{CB} of TiO_2 for efficient electron transfer. Recently, isoindigo-based D-π-A dyes were reported using TPA-iI-aryl structures also functionalized with cyanoacrylic acid.[56,57] In the first report of isoindigo-based DSSC dyes, the most efficient cell reached 6.0 % PCE and no use of TBP was reported.[56] TBP was used in a later study for similar iI-based D-π-A dyes, but the J_{sc} remained around 6 mA/cm^2 with limited efficiencies below 3.2 %.[57] Since the highest PCE reported among the series of iI-based dyes was 6.0%, isoindigo still appears to be a promising acceptor for metal-free DSSC dyes. Given its extended absorption, we believe this class of molecules would benefit from more in depth investigation regarding the key parameters that would limit DSSC efficiency, especially its low-lying LUMO energy level.[34]

D-A-D Structure. There is a large pool of conjugated molecules for bulk heterojunction solar cells and field effect transistors that have been designed as linear symmetrical D-A-D structures in order to control crystallization (symmetry) and HOMO/LUMO energy level tuning and energy gap reduction (D-A interaction).[14,15] Furthermore, many monomers used to synthesize D-A conjugated polymers are also of the D-A-D structure.[58] We find it surprising that the field of DSSCs has not investigated these simple, well characterized symmetrical structures in more detail, despite the possible energy misalignment compared to the typical D-π-A structure. To the best of our knowledge, this is the first report of such a D-A-D structure demonstrating high PCE in DSSCs (> 6%), as was found for T4BTD-A. Several studies of BTD containing dyes have been reported, some with excellent PCE reaching as high as 10%.[59−63] Still, all are based on a TPA-BTD-aryl-type structure functionalized with the commonly used cyanoacrylic acid anchoring group which would classify them as a D-π-A structure.

Color Control in D-A-D Conjugated Systems. When considering organic and hybrid photovoltaic systems for practical solar cells, one must examine the trade-offs in performance with conventional inorganic cells (high PCE) with the unique properties organic dyes can bring through solution processing, mechanically flexible cells, and aesthetically pleasing colors. In the context of the work here, this latter effect of the color is especially important as it opens up a variety of architectural (wall and window), automotive, and consumer device applications where the appearance of the solar cell is important. The dual band conjugated compounds[38] developed using the D-A-D molecular structure are especially conducive to this color control as the long wavelength charge transfer band can be moved across the visible spectrum to produce yellow, orange, red, magenta, and blue hues. By using strong electron acceptors, the dual band absorption can be red shifted such that the window of transmission moves into the 410−550 nm range inducing blue, cyan, and green hues to the systems.[16] This panchromatic selection of colors comes at the expense of some of the energy harvesting efficiency, but as the spectral response is broad, and can in all cases include the near infrared portion of the spectrum, this is not a debilitating problem. This is evident in the present work as the intensely red colored T4BTD-A with a transmission minimum at 420 nm (Figure 1) is the most efficient of the DSSCs studied. Colored DSSCs with transition metal complex based dyes have been developed to the point of near commercial viability.[2] Further evidence is seen in green colored polymer photovoltaic systems (green donor polymers blended with the acceptor $PC_{61}BM$ which has minimal visible light absorption), which can attain PCEs as high as 2.2 %.[64−67]

CONCLUSION

We reported the synthesis of metal-free dyes based on symmetrical D-A-D aromatic cores mono-functionalized with phosphonic acid anchoring groups designed to adsorb onto mesoporous TiO_2 films for DSSC application. The highest efficiency of 6.4 % was obtained for cells based on a benzothiadiazole acceptor within the D-A-D structure. We further investigated the limited performance of the dye based on the isoindigo acceptor by varying electrolyte composition: removing the TBP additive form the electrolyte led to a higher J_{sc} but lower V_{oc}, and increasing the LiI concentration exacerbated this effect. These results suggest that in our molecular design, the iI acceptor brought the LUMO level of the dye close to the conduction band of TiO_2. While it is commonly recognized that the D-π-A structure is the optimal design for DSSCs, this study demonstrates that molecules with D-A-D type electronic structures deserve to be investigated as sensitizers for DSSCs, not only based on the promising device performances reported herein, but also because the structure-property relationships of such constructs regarding color control and energy level tuning have been well characterized in the related fields of solid state organic photovoltaics and transistors.

ASSOCIATED CONTENT

Supporting Information

General synthetic details; synthetic procedures; additional figures. This material is available free of charge via the Internet at http://pubs.acs.org.

AUTHOR INFORMATION

Corresponding Authors

*Email: reynolds@chemistry.gatech.edu.
*Email: kschanze@chem.ufl.edu.

Notes

The authors declare no competing financial interest.

ACKNOWLEDGMENTS

The authors gratefully acknowledge the U.S. Department of Energy Solar Energy Technologies Program (DE-FG36-08GO18020) for financial support. R.S. acknowledges the University Alumni Awards Program for a fellowship.

REFERENCES

(1) O'Regan, B.; Grätzel, M. A Low-Cost, High-Efficiency Solar Cell Based on Dye-Sensitized Colloidal TiO_2 Films. *Nature* **1991**, *353*, 737−740.
(2) Hagfeldt, A.; Boschloo, G.; Sun, L.; Kloo, L.; Pettersson, H. Dye-Sensitized Solar Cells. *Chem. Rev.* **2010**, *110*, 6595−6663.
(3) Grätzel, M. Solar Energy Conversion by Dye-Sensitized Photovoltaic Cells. *Inorg. Chem.* **2005**, *44*, 6841−6851.
(4) Hardin, B. E.; Snaith, H. J.; McGehee, M. D. The Renaissance of Dye-Sensitized Solar Cells. *Nat. Photonics* **2012**, *6*, 162−169.

(5) Chen, C.-Y.; Wang, M.; Li, J.-Y.; Pootrakulchote, N.; Alibabaei, L.; Ngoc-le, C.; Decoppet, J.-D.; Tsai, J.-H.; Grätzel, C.; Wu, C.-G.; et al. Highly Efficient Light-Harvesting Ruthenium Sensitized for Thin-Film Dye-Sensitized Solar Cells. *ACS Nano* **2009**, *3*, 3103−3109.
(6) Li, L.-L.; Diau, E. W.-G. Porphyrin-Sensitized Solar Cells. *Chem. Soc. Rev.* **2013**, *42*, 291−304.
(7) Yella, A.; Lee, H.-W.; Tsao, H. N.; Yi, C.; Chandiran, A. K.; Nazeeruddin, M. K.; Diau, E. W.-G.; Yeh, C.-Y.; Zakeeruddin, S. M.; Grätzel, M. Porphyrin-Sensitized Solar Cells with Cobalt (II/III)-Based Redox Electrolyte Exceed 12 Percent Efficiency. *Science* **2011**, *334*, 629−634.
(8) Ragoussi, M.-E.; Ince, M.; Torres, T. Recent Advances in Phthalocyanine-Based Sensitizers for Dye-Sensitized Solar Cells. *Eur. J. Org. Chem.* **2013**, 6475−6489.
(9) Mishra, A.; Fischer, M. K. R.; Bäuerle, P. Metal-Free Organic Dyes for Dye-Sensitized Solar Cells: From Structure: Property Relationships to Design Rules. *Angew. Chem. Int. Ed.* **2009**, *48*, 2474−2499.
(10) Liang, M.; Chen, J. Arylamine Organic Dyes for Dye-Sensitized Solar Cells. *Chem. Soc. Rev.* **2013**, *42*, 3453−3488.
(11) Lee, M. M.; Teuscher, J.; Miyasaka, T.; Murakami, T. N.; Snaith, H. J. Efficient Hybrid Solar Cells Based on Meso-superstructured Organometal Halide Perovskites. *Science* **2012**, *338*, 643−647.
(12) Liu, M.; Johnston, M. B.; Snaith, H. J. Efficient Planar Heterojunction Perovskite Solar Cells by Vapor Deposition. *Nature* **2013**, *501*, 395−398.
(13) Burschka, J.; Pellet, N.; Moon, S.-J.; Humphry-Baker, R.; Gao, P.; Nazeeruddin, M. K.; Grätzel, M. Sequential Deposition as a Route to High-Performance Perovskite-Sensitized Solar Cells. *Nature* **2013**, *499*, 316−319.
(14) Walker, B.; Kim, C.; Nguyen, T.-Q. Small Molecule Solution-Processed Bulk Heterojunction Solar Cells. *Chem. Mater.* **2011**, *23*, 470−482.
(15) Wang, C.; Dong, H.; Hu, W.; Liu, Y.; Zhu, D. Semiconducting π-Conjugated Systems in Field-Effect Transistors: A Material Odyssey of Organic Electronics. *Chem. Rev.* **2012**, *112*, 2208−2267.
(16) Ellinger, S.; Graham, K. R.; Shi, P.; Farley, R. T.; Steckler, T. T.; Brookins, R. N.; Taranekar, P.; Mei, J.; Padilha, L. A.; Ensley, T. R.; et al. Donor−Acceptor−Donor-Based π-Conjugated Oligomers for Nonlinear Optics and Near-IR Emission. *Chem. Mater.* **2011**, 3805−3817.
(17) Péchy, P.; Rotzinger, F. P.; Nazeeruddin, M. K.; Kohle, O.; Zakeeruddin, S. M.; Humphry-Baker, R.; Grätzel, M. Preparation of Phosphonated Polypyridyl Ligands to Anchor Transition-Metal Complexes on Oxide Surfaces: Application for the Conversion of Light to Electricity with Nanocrystalline TiO_2 Films. *J. Chem. Soc., Chem. Commun.* **1995**, *369*, 65−66.
(18) Wang, P.; Klein, C.; Moser, J.-E.; Humphry-Baker, R.; Ngoc-le, C.; Charvet, R.; Comte, P.; Zakeeruddin, S. M.; Grätzel, M. Anchoring Ligand for Nanocrystalline Dye Sensitized Solar Cells. *J. Phys. Chem. B* **2004**, *35*, 17553−17559.
(19) Zabri, H.; Gillaizeau, I.; Bignozzi, C. A.; Caramori, S.; Charlot, M.-F.; Cano-Boquera, J.; Odobel, F. Synthesis and Comprehensive Characterizations of New *cis*-RuL_2X_2 (X = Cl, CN, and NCS) Sensitizers for Nanocrystalline TiO_2 Solar Cell Using Bis-Phosphonated Bipyridine Ligands (L). *Inorg. Chem.* **2003**, *42*, 6655−6666.
(20) Trammell, S. A.; Moss, J. A.; Yang, J. C.; Nakhle, B. M.; Slate, C. A.; Odobel, F.; Sykora, M.; Erickson, B. W.; Meyer, T. J. Sensitization of TiO_2 by Phosphonate-Derivatized Proline Assemblies. *Inorg. Chem.* **1999**, *38*, 3665−3669.
(21) Gillaizeau-Gauthier, I.; Odobel, F.; Alebbi, M.; Argazzi, R.; Costa, E.; Bignozzi, C. A.; Qu, P.; Meyer, G. J. Phosphonate-Based Bipyridine Dyes for Stable Photovoltaic Devices. *Inorg. Chem.* **2001**, *40*, 6073−6079.
(22) Zakeeruddin, S. M.; Nazeeruddin, M. K.; Péchy, P.; Rotzinger, F. P.; Humphry-Baker, R.; Kalyanasundaram, K.; Grätzel, M.; Shklover, V.; Haibach, T. Molecular Engineering of Photosensitizers for Nanocrystalline Solar Cells: Synthesis and Characterization of Ru Dyes Based on Phosphonated Terpyridines. *Inorg. Chem.* **1997**, *36*, 5937−5946.
(23) Houarner-Rassin, C.; Blart, E.; Buvat, P.; Odobel, F. Improved Efficiency of a Thiophene Linked Ruthenium Polypyridine Complex for Dry Dye-Sensitized Solar Cells. *J. Photochem. Photobiol., A* **2007**, *186*, 135−142.
(24) Houarner-Rassin, C.; Chaignon, F.; She, C.; Stockwell, D.; Blart, E.; Buvat, P.; Lian, T.; Odobel, F. Synthesis and Photoelectrochemical Properties of Ruthenium Bisterpyridine Sensitizers Functionalized with a Thienyl Phosphonic Acid Moiety. *J. Photochem. Photobiol., A* **2007**, *192*, 56−65.
(25) Bozic-Weber, B.; Constable, E. C.; Fürer, S. O.; Housecroft, C. E.; Troxler, L. J.; Zampese, J. A. Copper(I) Dye-Sensitized Solar Cells with $[Co(bpy)_3]^{(2+/3+)}$ Electrolyte. *Chem. Commun.* **2013**, *49*, 7222−7224.
(26) Neuthe, K.; Bittner, F.; Stiemke, F.; Ziem, B.; Du, J.; Zellner, M.; Wark, M.; Schubert, T.; Haag, R. Phosphonic Acid Anchored Ruthenium Complexes for ZnO-Based Dye-Sensitized Solar Cells. *Dye. Pigment.* **2014**, *104*, 24−33.
(27) Brennan, B. J.; Llansola Portolés, M. J.; Liddell, P. A.; Moore, T. A.; Moore, A. L.; Gust, D. Comparison of Silatrane, Phosphonic Acid, and Carboxylic Acid Functional Groups for Attachment of Porphyrin Sensitizers to TiO_2 in Photoelectrochemical Cells. *Phys. Chem. Chem. Phys.* **2013**, *15*, 16605−16614.
(28) Bedics, M. A.; Mulhern, K. R.; Watson, D. F.; Detty, M. R. Synthesis and Photoelectrochemical Performance of Chalcogenopyrylium Monomethine Dyes Bearing Phosphonate/Phosphonic Acid Substituents. *J. Org. Chem.* **2013**, *78*, 8885−8891.
(29) Mulhern, K. R.; Orchard, A.; Watson, D. F.; Detty, M. R. Influence of Surface-Attachment Functionality on the Aggregation, Persistence, and Electron-Transfer Reactivity of Chalcogenorhodamine Dyes on TiO_2. *Langmuir* **2012**, *28*, 7071−7082.
(30) Murakami, T. N.; Yoshida, E.; Koumura, N. Carbazole Dye with Phosphonic Acid Anchoring Groups for Long-Term Heat Stability of Dye-Sensitized Solar Cells. *Electrochim. Acta* **2013**, DOI: 10.1016/j.electacta.2013.12.013.
(31) Nilsing, M.; Persson, P.; Ojamäe, L. Anchor Group Influence on Molecule−Metal Oxide Interfaces: Periodic Hybrid DFT Study of Pyridine Bound to TiO_2 Via Carboxylic and Phosphonic Acid. *Chem. Phys. Lett.* **2005**, *415*, 375−380.
(32) Nilsing, M.; Persson, P.; Lunell, S.; Ojamäe, L. Dye-Sensitization of the TiO_2 Rutile (110) Surface by Perylene Dyes: Quantum-Chemical Periodic B3LYP Computations. *J. Phys. Chem. C* **2007**, *111*, 12116−12123.
(33) Queffélec, C.; Petit, M.; Janvier, P.; Knight, D. A.; Bujoli, B. Surface Modification Using Phosphonic Acids and Esters. *Chem. Rev.* **2012**, *112*, 3777−3807.
(34) Stalder, R.; Mei, J.; Graham, K. R.; Estrada, L. A.; Reynolds, J. R. Isoindigo, a Versatile Electron-Deficient Unit For High-Performance Organic Electronics. *Chem. Mater.* **2013**, *26*, 664−678.
(35) Stalder, R.; Xie, D.; Zhou, R.; Xue, J.; Reynolds, J. R.; Schanze, K. S. Variable-Gap Conjugated Oligomers Grafted to CdSe Nanocrystals. *Chem. Mater.* **2012**, *24*, 3143−3152.
(36) Nazeeruddin, M. K.; Péchy, P.; Renouard, T.; Zakeeruddin, S. M.; Humphry-Baker, R.; Comte, P.; Liska, P.; Cevey, L.; Costa, E.; Shklover, V.; et al. Engineering of Efficient Panchromatic Sensitizers for Nanocrystalline TiO_2-Based Solar Cells. *J. Am. Chem. Soc.* **2001**, *123*, 1613−1624.
(37) Wang, Z.-S.; Yamaguchi, T.; Sugihara, H.; Arakawa, H. Significant Efficiency Improvement of the Black Dye-Sensitized Solar Cell through Protonation of TiO_2 Films. *Langmuir* **2005**, *21*, 4272−4276.
(38) Beaujuge, P. M.; Amb, C. M.; Reynolds, J. R. Spectral Engineering in π-Conjugated Polymers with Intramolecular Donor−Acceptor Interactions. *Acc. Chem. Res.* **2010**, *43*, 1396−1407.
(39) Estrada, L. A.; Stalder, R.; Abboud, K. A.; Risko, C.; Brédas, J.-L.; Reynolds, J. R. Understanding the Electronic Structure of Isoindigo in Conjugated Systems: A Combined Theoretical and Experimental Approach. *Macromolecules* **2013**, *46*, 8832−8844.

(40) Pavlishchuk, V. V.; Addison, A. W. Conversion Constants for Redox Potentials Measured Versus Different Reference Electrodes in Acetonitrile Solutions at 25 °C. *Inorg. Chim. Acta* **2000**, *298*, 97−102.
(41) Hansen, W. N.; Hansen, G. J. Absolute Half-Cell Potential: A Simple Direct Measurement. *Phys. Rev. A* **1987**, *36*, 1396−1402.
(42) Cardona, C. M.; Li, W.; Kaifer, A. E.; Stockdale, D.; Bazan, G. C. Electrochemical Considerations for Determining Absolute Frontier Orbital Energy Levels of Conjugated Polymers for Solar Cell Applications. *Adv. Mater.* **2011**, *23*, 2367−2371.
(43) Ronca, E.; Pastore, M.; Belpassi, L.; Tarantelli, F.; De Angelis, F. Influence of the Dye Molecular Structure on the TiO_2 Conduction Band in Dye-Sensitized Solar Cells: Disentangling Charge Transfer and Electrostatic Effects. *Energy Environ. Sci.* **2013**, *6*, 183−193.
(44) Kalyanasundaram, K.; Grätzel, M. Applications of Functionalized Transition Metal Complexes in Photonic and Optoelectronic Devices. *Coord. Chem. Rev.* **1998**, *77*, 347−414.
(45) Grätzel, M. Photoelectrochemical Cells. *Nature* **2001**, *414*, 338−344.
(46) Chung, I.; Lee, B.; He, J.; Chang, R. P. H.; Kanatzidis, M. G. All-Solid-State Dye-Sensitized Solar Cells with High Efficiency. *Nature* **2012**, *485*, 486−489.
(47) Ambrosio, F.; Martsinovich, N.; Troisi, A. Effect of the Anchoring Group on Electron Injection: Theoretical Study of Phosphonated Dyes for Dye-Sensitized Solar Cells. *J. Phys. Chem. C* **2012**, *116*, 2622−2629.
(48) Cho, C.-P.; Chu, C.-C.; Chen, W.-T.; Huang, T.-C.; Tao, Y.-T. Molecular Modification on Dye-Sensitized Solar Cells by Phosphonate Self-Assembled Monolayers. *J. Mater. Chem.* **2012**, *22*, 2915−2921.
(49) Boschloo, G.; Häggman, L.; Hagfeldt, A. Quantification of the Effect of 4-*tert*-Butylpyridine Addition to I^-/I^{3-} Redox Electrolytes in Dye-Sensitized Nanostructured TiO_2 Solar Cells. *J. Phys. Chem. B* **2006**, *110*, 13144−13150.
(50) Tang, J.; Wu, W.; Hua, J.; Li, J.; Li, X.; Tian, H. Starburst Triphenylamine-Based Cyanine Dye for Efficient Quasi-Solid-State Dye-Sensitized Solar Cells. *Energy Environ. Sci.* **2009**, *2*, 982−990.
(51) Johansson, P. G.; Rowley, J. G.; Taheri, A.; Meyer, G. J.; Singh, S. P.; Islam, A.; Han, L. Long-Wavelength Sensitization of TiO_2 by Ruthenium Diimine Compounds with Low-Lying π^* Orbitals. *Langmuir* **2011**, *27*, 14522−14531.
(52) Yanagida, M.; Yamaguchi, T.; Kurashige, M.; Hara, K.; Katoh, R.; Sugihara, H.; Arakawa, H. Panchromatic Sensitization of Nanocrystalline TiO_2 with *cis*-Bis(4-carboxy-2-[2′-(4′-carboxypyridyl)]quinoline)bis(thiocyanato-N)ruthenium(II). *Inorg. Chem.* **2003**, *42*, 7921−7931.
(53) Redmond, G.; Fitzmaurice, D. Spectroscopic Determination of Flatband Potentials. *J. Phys. Chem.* **1993**, *97*, 1426−1430.
(54) Liu, Y.; Hagfeldt, A.; Xiao, X.-R.; Lindquist, S.-E. Investigation of Influence of Redox Species on the Interfacial Energetics of a Dye-Sensitized Nanoporous TiO_2 Solar Cell. *Sol. Energy Mater. Sol. Cells* **1998**, *55*, 267−281.
(55) Mathew, A.; Anand, V.; Rao, G. M.; Munichandraiah, N. Effect of Iodine Concentration on the Photovoltaic Properties of Dye Sensitized Solar Cells for Various I_2/LiI Ratios. *Electrochim. Acta* **2013**, *87*, 92−96.
(56) Ying, W.; Guo, F.; Li, J.; Zhang, Q.; Wu, W.; Tian, H.; Hua, J. Series of New D-A-π-A Organic Broadly Absorbing Sensitizers Containing Isoindigo Unit for Highly Efficient Dye-Sensitized Solar Cells. *ACS Appl. Mater. Interfaces* **2012**, *4*, 4215−4224.
(57) Gang, W.; Haijun, T.; Yiping, Z.; Yingying, W.; Zhubin, H.; Guipeng, Y.; Chunyue, P. Series of D-π-A System Based on Isoindigo Dyes for DSSC: Synthesis, Electrochemical, and Photovoltaic Properties. *Synth. Met.* **2014**, *187*, 17−23.
(58) Cheng, Y.-J.; Yang, S.-H.; Hsu, C.-S. Synthesis of Conjugated Polymers for Organic Solar Cell Applications. *Chem. Rev.* **2009**, *109*, 5868−5923.
(59) Chou, H.-H.; Chen, Y.-C.; Huang, H.-J.; Lee, T.-H.; Lin, J. T.; Tsai, C.; Chen, K. High-Performance Dye-Sensitized Solar Cells Based on 5,6-Bis-hexyloxy-benzo[2,1,3]thiadiazole. *J. Mater. Chem.* **2012**, *22*, 10929−10938.
(60) Tang, Z.-M.; Lei, T.; Jiang, K.-J.; Song, Y.-L.; Pei, J. Benzothiadiazole Containing D-π-A Conjugated Compounds for Dye-Sensitized Solar Cells: Synthesis, Properties, and Photovoltaic Performances. *Chem. - Asian J.* **2010**, *5*, 1911−1917.
(61) Kim, J.-J.; Choi, H.; Lee, J.-W.; Kang, M.-S.; Song, K.; Kang, S. O.; Ko, J. A Polymer Gel Electrolyte to Achieve ≥6% Power Conversion Efficiency with a Novel Organic Dye Incorporating a Low-Band-Gap Chromophore. *J. Mater. Chem.* **2008**, *18*, 5223−5229.
(62) Zhu, W.; Wu, Y.; Wang, S.; Li, W.; Li, X.; Chen, J.; Wang, Z.; Tian, H. Organic D-A-π-A Solar Cell Sensitizers with Improved Stability and Spectral Response. *Adv. Funct. Mater.* **2011**, *21*, 756−763.
(63) Wu, Y.; Marszalek, M.; Zakeeruddin, S. M.; Zhang, Q.; Tian, H.; Grätzel, M.; Zhu, W. High-Conversion-Efficiency Organic Dye-Sensitized Solar Cells: Molecular Engineering on D-A-π-A Featured Organic Indoline Dyes. *Energy Environ. Sci.* **2012**, *5*, 8261−8272.
(64) Subbiah, J.; Beaujuge, P. M.; Choudhury, K. R.; Ellinger, S.; Reynolds, J. R.; So, F. Efficient Green Solar Cells Via a Chemically Polymerizable Donor-Acceptor Heterocyclic Pentamer. *ACS Appl. Mater. Interfaces* **2009**, *1*, 1154−1158.
(65) Amb, C. M.; Craig, M. R.; Koldemir, U.; Subbiah, J.; Choudhury, K. R.; Gevorgyan, S. A.; Jørgensen, M.; Krebs, F. C.; So, F.; Reynolds, J. R. Aesthetically Pleasing Conjugated Polymer/Fullerene Blends for Blue-Green Solar Cells Via Roll-to-Roll Processing. *ACS Appl. Mater. Interfaces* **2012**, *4*, 1847−1853.
(66) Inganäs, O.; Zhang, F.; Andersson, M. R. Alternating Polyfluorenes Collect Solar Light in Polymer Photovoltaics. *Acc. Chem. Res.* **2009**, *42*, 1731−1739.
(67) Zhang, F.; Mammo, W.; Andersson, L. M.; Admassie, S.; Andersson, M. R.; Inganäs, O. Low-Bandgap Alternating Fluorene Copolymer/Methanofullerene Heterojunctions in Efficient Near-Infrared Polymer Solar Cells. *Adv. Mater.* **2006**, *18*, 2169−2173.